WELDED JOINTS

JOINING FE55006 CAST IRON AND SAE 8620 STEEL BY FRICTION HYDRO-PILLAR PROCESSING (FHPP)

Renan Mensch Landell,[1] Thiago Tauchen Rossatto,[1] Diogo Trento Buzzatti,[1] Guilherme Vieira Braga Lemos,[1, 3] Cleber Rodrigo De Lima Lessa,[2] Daniel Saraiva,[1] Douglas Martinazzi,[1] and Afonso Reguly[1]

The possibility of using a special type of Friction Stir Welding (FSW) – Friction Hydro Pillar Processing (FHPP) to manufacture a joining between dissimilar materials (high-carbon ductile iron FE55006 and low-carbon steel SAE 8620) is studied. The macrostructure, microstructure, microhardness and residual stresses of the welded joint are determined. The efficiency of using the FHPP technology for obtaining high-quality joints from dissimilar iron-based alloys is demonstrated. It is established that such joints have a high hardness due to the formation of a martensitic structure in the alloys during their processing by the FHPP method.

Key words: friction stir welding, friction hydro-pillar processing, high-carbon ductile cast iron, low-carbon structural steel, microstructure, residual stresses.

INTRODUCTION

Ductile cast irons (DCI) are characterized by presence of nodular or spheroidal graphite inclusions, which make them more ductile as compared to white cast irons. Ductile cast irons are used in the automotive industry to make crank-shafts, gearboxes, wheel hubs, disk brake calipers, engine connecting rids, structural turbine parts etc. [1]. In accordance with [2], a wind turbine employs from 15 to 25 tons DCI due to the suitable mechanical properties. In some cases, the combination of the ductility, impact toughness, strength, and hot deformability makes the DCI comparable to steels at a lower cost and density [2 – 4]. For this reason, some authors have considered the possibility of joining cast irons to other alloys.

Arc welding of cast irons is a challenge due to their high carbon equivalent (C^{eq}), which usually amounts to from 3.5 to 5.0% [5]. In this case, the structure of the DCI can acquire brittle phases and transform into a white iron depending on the temperature and the cooling rate under the welding [5]. In addition, different alloys have different meting temperatures and properties, which makes any welding process hard to conduct. Some researchers [6] have studied the weldability of vermicular cast iron using various electrodes. After such welding, the structure in the heat-affected zone (HAZ) may contain hard phases and cracks depending on the electrode used. Difficulties with fusion welding of high-strength DCI (σ_r = 700 MPa) have been reported in [7]. Nondestructive inspection of these welded joints shows presence of porous regions, undercuts and small cracks, and they are rejected. The post-weld heat treatment provides in such joints a σ_r = 399 MPa. In [8], diffusion welding is applied to obtain a

[1] Laboratório de Metalurgia Física (LAMEF); Programa de Pós Graduação em Engenharia de Minas, Metalúrgica e de Materiais (PPGE3M); Universidade Federal do Rio Grande do Sul (UFRGS), Porto Alegre, Brasil.

[2] Universidade Federal de Santa Maria (UFSM), Campus Cachoeira do Sul, RS, Brasil; Programa de Pós-Graduaçãoem Tecnologia e Engenharia de Materiais (PPG-TEM) do Instituto Federal do Rio Grande do Sul (IFRS), Caxias do Sul, Brasil.

[3] E-mail: guilherme.lemos@ufrgs.br

TABLE 1. Chemical Compositions of Materials Studied

Alloy	Content of chemical elements, wt.%									
	C	Si	Mn	S	Cr	Ni	Cu	Mg	Al	Fe
DCI FE55006	> 2.100	0.690	0.045	0.119	0.009	< 0.005	< 0.010	0.006	0.006	Base
Steel SAE 8620	0.175	0.221	0.805	0.010	0.455	0.400	0.214	< 0.010	0.023	Base

welded joint of a DCI and a martensitic stainless steel. The mechanical properties of the joint are optimized by raising the temperature of the process to 1100°C.

With allowance for the problems arising in arc welding of cast irons, it is expedient to study the possibility of friction welding for these materials due to the solid-phase nature of the process and reduced heat input. In addition, friction welding can be used for forming welded joints of dissimilar materials, which is hard or impossible in arc welding [9]. The friction welding process is based on the heat generated by the friction, which creates a hot plasticized state, which makes it possible to join and mix the alloys [10, 11]. Since the process is conducted at a temperature below the melting point, it is possible to provide lower changes in the microstructure and elevation of the mechanical properties. In [3], friction welding has been used to obtain a joint between a DCI and stainless steel AISI 321. The process was accompanied by interdiffusion of the alloys, enrichment of the iron with Cr and Ni, and migration of carbon from the DCI into the stainless steel. These processes produced chromium carbides on grain boundaries [3]. The microstructure of a joint of a DCI and carbon steel has been studied in [12]. The microstructure of the interface had four different-nature regions containing (i) inclusions of spheroidal graphite with the same diameter as in the original iron, (ii) ferrite, pearlite and refined graphite inclusions, (iii) only pearlite, and (iv) pearlite and ferrite resembling those contained in the original steel. The microstructure of a 12-mm plate from pure ductile iron has been analyzed in [13] after friction stir processing. The changes in the microstructure of the joint consisted mainly in disintegration of the grains. In [14], rods with diameter 20 mm from aluminum alloy AA1050 have been welded to DCI by rotary friction welding, and the interface was analyzed. The periphery of the rod acquired a high content of Fe_xAl_y intermetallic, which reduced the σ_r.

The aim of the present work was to assess the possibility of the use of friction hydro-pillar processing (FHPP), which a variant of friction stir welding, for creating a joint between dissimilar materials, i.e., high-carbon ductile cast iron FE55006 (KCh55-4) and low-carbon steel SAE 8620 (20KhGNM), and to study the structure and the properties of the welded joint obtained.

METHODS OF STUDY

We studied ductile cast iron FE55006 and steel SAE 8620 subjected to friction hydro-pillar processing (FHPP) in an MPF 1000 facility (developed by LAMEF/UFRGS). The chemical compositions of the alloys, i.e., of the consumable rods (the cast iron) and the base material (the steel), determined with the help of an optical emission spectrometer are presented in Table 1. It should be noted that the difference in the carbon contents of the materials was considerable (the DCI contained 12 times more carbon than the steel). The sizes of the parts were taken from [15].

To make the samples for the macro- and microstructural analysis, the weld was cut; the sections were prepared by the standard metallographic procedures and etched with 10% nital. The local mechanical properties were determined by measuring the microhardness at a load of 300 g; the distance between the indents was 0.2 mm. The macro- and microstructures of different parts of the joint were compared with allowance for the corresponding values of the microhardness.

The residual stresses in the FHPP joint were assessed by drilling holes. The procedure was taken from the ASTM E837 [16]. The residual stresses were calculated by the method of Kockkelmann [17]. We made three measurements in each region, i.e., in the base metal from steel SAE 8620, in the pin (rod) from iron FE55006 and at their interface. Thus, the residual stresses were determined over cross sections of the joint at a distance of 0.08 – 0.80 mm from the weld. The scheme of the determination of the residual stresses is presented in Fig. 1.

RESULTS AND DISCUSSION

The microstructures of the welded cast iron and steel in the initial condition are presented in Fig. 2. The microstructure of the rod (FE55006) is represented by spheroidal graphite inclusions of different sizes and pearlite islands in a ferrite matrix. The microstructure of the base metal (SAE 8620) consists of proeutectiod ferrite and pearlite.

Figure 3 presents the results of the measurement of the microhardness over cross section of the welded joint and the macrostructure of joint. The location of the regions studied in the welded joint is given in Fig. 3a; Fig. 3b – f give their microstructure at a higher magnification. The darker areas of the microstructure correspond to the DCI and the lighter ones correspond to SAE 8620.

The microstructure in Fig. 3b contains acicular ferrite (AF), ferrite (F) and bainite (B); its microhardness attains about 257 HV. Figure 3c presents the microstructure containing B, AF, and Widmanstatten ferrite (W) with microhard-
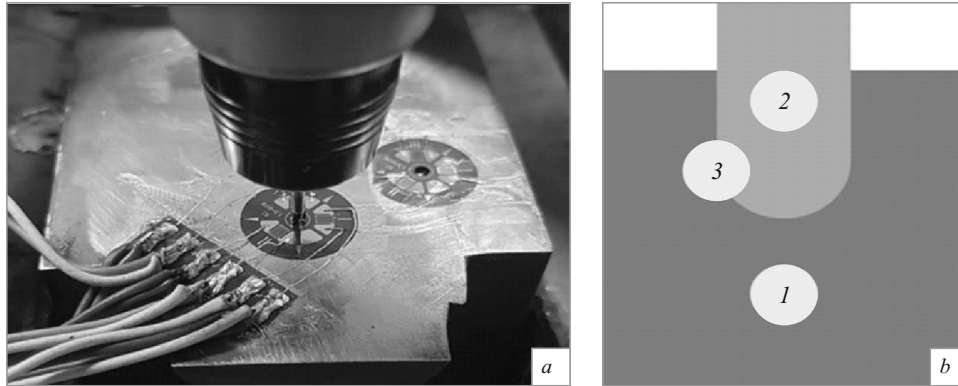
Fig. 1. Method of assessment of residual stresses: *a*) device for drilling holes; *b*) scheme of location of measured regions; *1*) base metal (steel SAE 8620); *2*) pin (cast iron FE55006); *3*) interface.
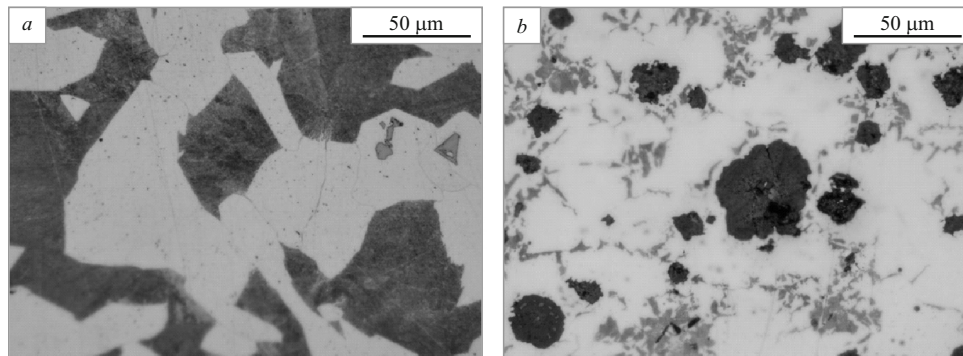
Fig. 2. Microstructures of welded alloys in initial condition: *a*) steel SAE 8620; *b*) cast iron FE55006.

ness about 300 *HV*. The microstructure of the interface (Fig. 3*d*) consists primarily of martensite (M), W, and B. In this zone, the thermomechanical impact has produced a thin white layer with a hardness of about 700 *HV*, which may be associated with the presence of martensite and its high hardness. The intense plastic deformation gives rise to high friction and local superheating of the metal above Ar_{cm} (the critical value for the transformation in cooling). When the FHPP is stopped, the high rate of cooling below M_s (the temperature of the start of martensitic transformation) causes formation of martensite. Figure 3*e* presents the microstructure containing M, B, P (pearlite) and G (graphite) and having a microhardness of 400 *HV*. Closer to the center of the pin (Fig. 3*f*) the microstructure is represented by B, P, F, and G.

The results of the measurement of residual stresses in different regions of the FHPP joint are presented in Fig. 4. The figure gives maximum and minimum stresses in the base material (steel SAE 8620), in the pin material (cast iron FE55006) and at their interface. Near the surface (at distance $h = 0.08$ mm) the maximum residual stresses in SAE 8629 are close to 50 MPa, i.e., are low tensile stresses. At the interface, the maximum residual stresses vary from –25 to –48 MPa depending on the distance h. In the pin material

(FE55006) the maximum residual stresses vary from 25 to 140 MPa, which is explainable by their correlation with the microhardness of the metal [18].

The values of the minimum residual compressive stresses at the interface attain –128 MPa. In the base metal (SAE 8620) the minimum residual stresses remain virtually invariable over the thickness (–25 MPa). Moreover, the material of the pin (FE55006) also acquires residual compressive stresses of up to –70 MPa. Consequently, the assessment of the residual stresses shows that the transition region of the interface undergoes the highest residual compressive stresses (up to –128 MPa), which agrees with the data of other authors calculated by the finite-element method [19, 20].

CONCLUSIONS

We have performed experimental studies of the structure and properties of a welded joint of high-carbon ductile cast iron FE55006 and low-carbon steel SAE 8620 created by friction hydro-pillar processing (FHPP). It has been shown that it is possible in principle to use friction hydrostatic processing for joining dissimilar materials. The welded joint obtained is characterized by inhomogeneous microstructure,
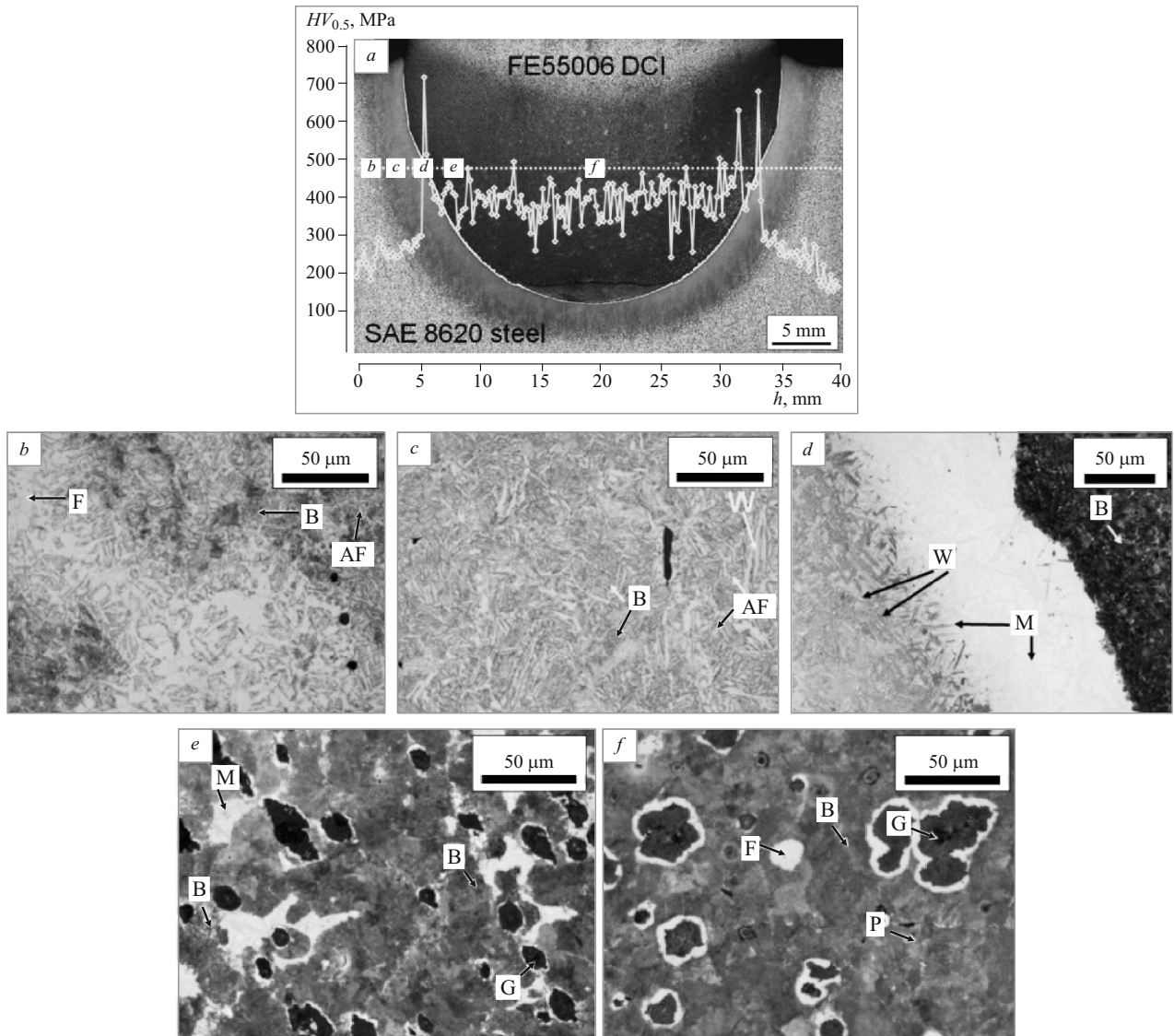
Fig. 3. General view and microhardness $HV_{0.5}$ of FHPP welded joint of cast iron FE55006 and steel SAE9620 (*a*) and microstructure (*b – f*) of its regions (their location is presented in Fig. 3*a*): *h*) distance from the start of microhardness measurement (in the base metal); AF) acicular ferrite; F) ferrite; B) bainite; W) Widmanstatten ferrite; M) martensite; P) pearlite.
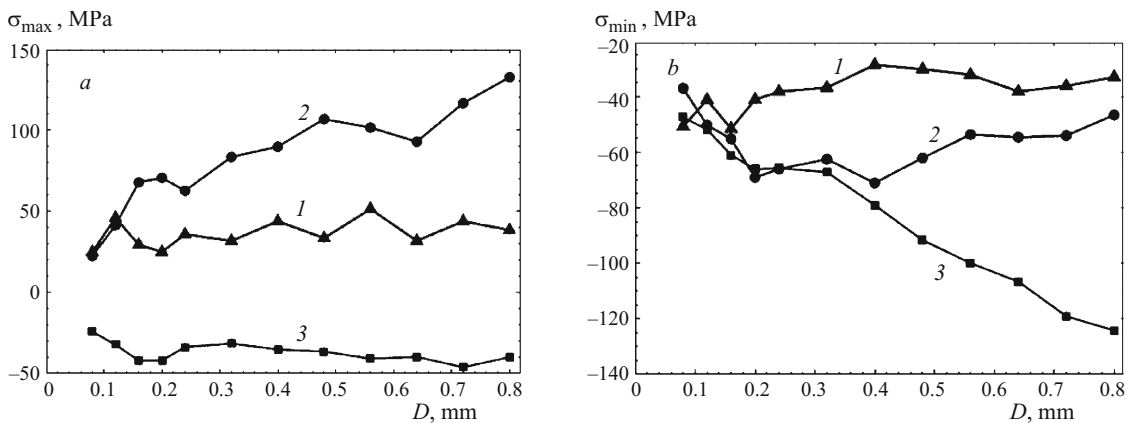
Fig. 4. Variation of tensile (*a*) and compressive (*b*) residual stresses over the depth *D* of different regions in welded joint of cast iron FE55006 and steel SAE 8620 formed by FHPP: *1*) base material SAE 8620; *2*) pin material FE55006; *3*) interface.

microhardness, and level of residual stresses in different regions. A thin white layer with the highest microhardness (about 700 HV) containing martensite produced by severe plastic deformation is formed at the interface of the base metal (the steel) and the pin (the ductile cast iron). This region also exhibits maximum residual compressive stresses (up to –128 MPa).

REFERENCES

1. S. Korkmaz, "A methodology to predict fatigue life of cast iron: uniform material law for cast iron," *J. Iron Steel Res. Int.*, **18**(8), 42 – 45 (2011).

2. M. Shirani and G. Härkegård, "Fatigue life distribution and size effect in ductile cast iron for wind turbine components," *Eng. Fail. Anal.*, **18**(1), 12 – 24 (2011).

3. R. Winiczenko and M. Kaczorowski, "Friction welding of ductile iron with stainless steel," *J. Mater. Process. Technol.*, **213**(3), 453 – 462 (2013).

4. R. A. Bushey, "Welding of cast irons," in: *ASM Handbook, Vol. 6. Welding, Brazing, and Soldering*, ASM International, (1993), pp. 708 – 721.

5. A. Zeemann, *A Soldagem por Fusão Para Reconstruçãode Componentes de Ferro Fundido*, Infosolda (2003), pp. 1 – 4.

6. R. A. Lovato, W. Guesser, and A. F. Paris, "Soldagem de ferro fundido vermicular com eletrodos revestidos (Welding Compacted Iron with SMAW)" in: *Congresso Nacional de Soldagem, Caxias do Sul. Anais. Abs.* (2007), V. 32, p. 1.

7. L. A. Pereira, "Estudo da soldabilidade do ferro fundido dúctil SiboDur® 700," 159 f.: *Dissertação de Mestrado. Engenharia Mecânica*, Instituto Superior de Engenharia do Porto, Porto (2016).

8. S. Kolukisa, "The effect of the welding temperature on the weldability in diffusion welding of martensitic (AISI 420) stainless steel with ductile (spheroidal graphite-nodular) cast iron," *J. Mater. Process. Technol.*, **186**(1 – 3), 33 – 36 (2007).

9. *International Organization for Standardization. ISO 15620: Welding – Friction Welding of Metallic Materials*, ISO, Switzerland (2000), 33 p.

10. A. Meyer, "Friction hydro pillar processing: bonding mechanism and properties," in: *Master thesis. Gemeinsamen Fakultät für Maschinenbau und Elektrotechnik Der Technischen Universität Carolo*, Braunschweig (2004), 135 p.

11. S. Yu. Kondrat'ev, Yu. N. Morozova, Yu. A. Golubev et al., "Microstructure and mechanical properties of welds of Al – Mg – Si alloys after different modes of impulse friction stir welding," *Met. Sci. Heat Treat.*, **59**(11 – 12), 697 – 702 (2018).

12. R. Ueji, "Microstructure evolution in dissimilar metal joint interface obtained by friction welding of cast iron and carbon steel," *Join. Weld. Res. Inst.*, Osaka, **42**(1), 33 – 37 (2013).

13. S. Mironov, Y. Sato, and H. Kokawa, "Microstructural evolution during friction stir-processing of pure iron," *Acta Mater.*, **56**(11), 2602 – 2614 (2008).

14. Yu-lai Song, et al., Strength distribution at interface of rotary-friction-welded aluminum to nodular cast iron," *Trans. Nonferr. Met. Soc. China*, **18**(1), 14 – 18 (2008)

15. D. Martinazzi, G. V. B. Lemos, R. M. Landell, et al., "Estudo preliminar sobre o efeito da geometria do pino no processo de soldagem FHPP entre o ferro fundido nodular FE55006 e o aço SAE 8620," *Periódico Tchê Química*, **16**(31), 642 (2019).

16. *ASTM E-837. Standard Test Method for Determining Residual Stresses by the Hole-Drilling Strain-Gage Method, Annual Book of ASTM Standards, Vol. 03.01*, ASTM International (2002), 16 p.

17. T. Schwarz and H. Kockkelmann, *The Hole-Drilling Method — the Best Technique for the Experimental Determination of Residual Stress in Many Fields of Application*, MTB, Stuttgart (1993), pp. 33 – 38.

18. S. Gencalp Irizalp, N. Saklakoglu, F. Baris, and S. Kayral, "Effect of shot peening on residual stress distribution and microstructure evolution of artificially defected 50CrV4 steel," *J. Mater. Eng. Perform.*, **29**(11), 7607 – 7616 (2020).

19. S. K. Singh, K. Chattopadhyay, and P. Dutta, "Determination of optimum process parameters and residual stress in friction welding of thixocast A356 aluminum alloy," *Metall. Mater. Trans. B*, **51**(6), 3079 – 3088 (2020).

20. C. Bühr, B. Ahmad, P. A. Colegrove, et al., "Prediction of residual stress within linear friction welds using a computationally efficient modelling approach," *Mater. Des.*, **139**, 222 – 233 (2018).